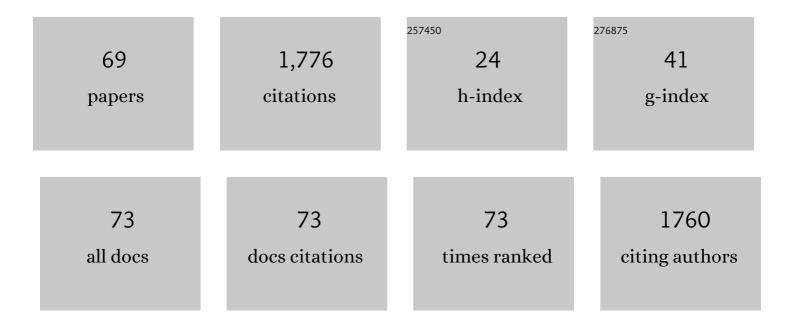
Guillaume Bernard-Granger

List of Publications by Year in descending order

Source: https://exaly.com/author-pdf/3631277/publications.pdf Version: 2024-02-01



#	Article	IF	CITATIONS
1	Multi-scale homogeneity analysis of co-milled powders: Development of a reverse approach to assess quality of mixtures. Powder Technology, 2022, 400, 117263.	4.2	1
2	Y-TZP, Ce-TZP and as-synthesized Ce-TZP/Al2O3 materials in the development of high loading rate digital light processing formulations. Ceramics International, 2021, 47, 3892-3900.	4.8	6
3	Predicting the flowability of powder mixtures from their single components properties through the multi-component population-dependent granular bond number; extension to ground powder mixtures. Powder Technology, 2021, 379, 26-37.	4.2	5
4	Investigating grinding mechanisms and scaling criteria in a ball mill by dimensional analysis. Advanced Powder Technology, 2021, 32, 2988-3001.	4.1	3
5	Predicting the flowability of alumina powder during batch grinding through the establishment of a grinding kinetic model. Advanced Powder Technology, 2021, 32, 3207-3219.	4.1	2
6	Influence of the PuO2 content on the sintering behaviour of UO2-PuO2 freeze-granulated powders under reducing conditions. Journal of the European Ceramic Society, 2021, 41, 6778-6783.	5.7	3
7	Sintering of a UO2-PuO2 freeze-granulated powder under reducing conditions. Journal of the European Ceramic Society, 2020, 40, 5900-5908.	5.7	6
8	Transmission Electron Microscopy Investigations on a Polysiloxane Preceramic Polymer Pyrolyzed at High Temperature in Argon. Ceramics, 2020, 3, 421-427.	2.6	4
9	Sintering investigations of a UO2-PuO2 powder synthesized using the freeze-granulation route. Scripta Materialia, 2020, 186, 190-195.	5.2	5
10	Dense and homogeneous MOX fuel pellets manufactured using the freeze granulation route. Journal of the American Ceramic Society, 2020, 103, 3020-3029.	3.8	8
11	Impact of fine particles on the rheological properties of uranium dioxide powders. Nuclear Engineering and Technology, 2020, 52, 1714-1723.	2.3	12
12	Investigation of a granular Bond number based rheological model for polydispersed particulate systems. Chemical Engineering Science, 2020, 228, 115971.	3.8	7
13	Fabrication of homogenous pellets by freeze granulation of optimized TiO2-Y2O3 suspensions. Journal of the European Ceramic Society, 2019, 39, 2168-2178.	5.7	15
14	Rheological properties of alumina powder mixtures investigated using shear tests. Powder Technology, 2019, 345, 300-310.	4.2	7
15	Sintering Ce-TZP/alumina composites using aluminum isopropoxide as a precursor. Ceramics International, 2019, 45, 10530-10540.	4.8	5
16	Preparation and co-dispersion of TiO2-Y2O3 suspensions through the study of their rheological and electrokinetic properties. Ceramics International, 2019, 45, 3023-3032.	4.8	8
17	Influence of the addition of HfO 2 particles on the thermoelectric properties of an N-type half-Heusler alloy sintered by spark plasma sintering. Journal of Alloys and Compounds, 2017, 709, 36-41.	5.5	9
18	Growth and thermal properties of doped monocrystalline titanium-silicide based quantum dot superlattices. Superlattices and Microstructures, 2016, 92, 249-255.	3.1	5

#	Article	IF	CITATIONS
19	Monocrystalline molybdenum silicide based quantum dot superlattices grown by chemical vapor deposition. Superlattices and Microstructures, 2016, 97, 341-345.	3.1	4
20	Microstructure investigations and thermoelectric properties of an N-type Half-Heusler alloy sintered by spark plasma sintering. Scripta Materialia, 2016, 123, 100-104.	5.2	9
21	Effect of microstructure on the thermal conductivity of nanostructured Mg2(Si,Sn) thermoelectric alloys: An experimental and modeling approach. Acta Materialia, 2015, 95, 102-110.	7.9	43
22	Microstructure investigations and thermoelectrical properties of an N-type magnesium–silicon–tin alloy sintered from a gas-phase atomized powder. Acta Materialia, 2015, 96, 437-451.	7.9	19
23	Assessment of ultrathin yttria-stabilized zirconia foils for biomedical applications. Journal of Materials Science, 2015, 50, 6197-6207.	3.7	9
24	Influence of the addition of Half-Heusler nanoparticles on the thermoelectrical properties of an N-type magnesium–silicon–tin alloy. Scripta Materialia, 2015, 104, 5-8.	5.2	5
25	High-Performance Silicon–Germanium-Based Thermoelectric Modules for Gas Exhaust Energy Scavenging. Journal of Electronic Materials, 2015, 44, 2192-2202.	2.2	40
26	Titanium-based silicide quantum dot superlattices for thermoelectrics applications. Nanotechnology, 2015, 26, 275605.	2.6	13
27	Microstructure investigations and thermoelectrical properties of a P-type polycrystalline higher manganese silicide material sintered from a gas-phase atomized powder. Journal of Alloys and Compounds, 2015, 618, 403-412.	5.5	37
28	Thermoelectric properties of an N-type silicon–germanium alloy related to the presence of silica nodules dispersed in the microstructure. Scripta Materialia, 2014, 93, 40-43.	5.2	6
29	Influence of in situ formed MoSi2 inclusions on the thermoelectrical properties of an N-type silicon–germanium alloy. Acta Materialia, 2014, 64, 429-442.	7.9	36
30	Microstructure and thermoelectrical investigations of an N-type magnesium–silicon–tin alloy. Journal of Alloys and Compounds, 2014, 598, 272-277.	5.5	10
31	Growth and characterization of QDSL (Quantum Dots Superlattices) of metal silicides in an n-doped SiGe matrix for thermoelectric applications. , 2014, , .		2
32	Stabilization of the tetragonal phase in large columnar zirconia crystals without incorporating dopants. Scripta Materialia, 2013, 68, 559-562.	5.2	12
33	Influence of nanosized inclusions on the room temperature thermoelectrical properties of a p-type bismuth–tellurium–antimony alloy. Acta Materialia, 2012, 60, 4523-4530.	7.9	8
34	A comparative study of Spark Plasma Sintering (SPS), Hot Isostatic Pressing (HIP) and microwaves sintering techniques on p-type Bi2Te3 thermoelectric properties. Materials Research Bulletin, 2012, 47, 1954-1960.	5.2	74
35	Spark plasma sintering of a p-type Si1â^'x Ge x alloy: identification of the densification mechanism by isothermal and anisothermal methods. Journal of Materials Science, 2012, 47, 4313-4325.	3.7	12
36	Sintering of an Ultrapure αâ€Alumina Powder: II. Mechanical, Thermoâ€Mechanical, Optical Properties, and Missile Dome Design. International Journal of Applied Ceramic Technology, 2011, 8, 366-382.	2.1	8

#	Article	IF	CITATIONS
37	Sintering Analysis of a Fine-Grained Alumina-Magnesia Spinel Powder. Journal of the American Ceramic Society, 2011, 94, 1388-1396.	3.8	34
38	Sintering of Soda‣ime Glass Microspheres Using Spark Plasma Sintering. Journal of the American Ceramic Society, 2011, 94, 2926-2932.	3.8	20
39	Influence of surface tension, osmotic pressure and pores morphology on the densification of ice-templated ceramics. Journal of the European Ceramic Society, 2011, 31, 983-987.	5.7	39
40	Spark plasma sintering of a commercially available granulated zirconia powder: Comparison with hot-pressing. Acta Materialia, 2010, 58, 3390-3399.	7.9	90
41	Sintering of a quasi-crystalline powder using spark plasma sintering and hot-pressing. Acta Materialia, 2010, 58, 5120-5128.	7.9	38
42	Superplasticity of a Fineâ€Grained TZ3Y Material Involving Dynamic Grain Growth and Dislocation Motion. Journal of the American Ceramic Society, 2010, 93, 848-856.	3.8	8
43	Densification mechanism involved during spark plasma sintering of a codoped α-alumina material: Part I. Formal sintering analysis. Journal of Materials Research, 2009, 24, 179-186.	2.6	41
44	Phenomenological analysis of densification mechanism during spark plasma sintering of MgAl ₂ O ₄ . Journal of Materials Research, 2009, 24, 2011-2020.	2.6	33
45	Influence of graphite contamination on the optical properties of transparent spinel obtained by spark plasma sintering. Scripta Materialia, 2009, 60, 164-167.	5.2	132
46	Inversion defects in MgAl2O4 elaborated by pressureless sintering, pressureless sintering plus hot isostatic pressing, and spark plasma sintering. Scripta Materialia, 2009, 61, 516-519.	5.2	5
47	Metastable and unstable cellular solidification of colloidal suspensions. Nature Materials, 2009, 8, 966-972.	27.5	201
48	Spark plasma sintering of a commercially available granulated zirconia powder—II. Microstructure after sintering and ionic conductivity. Acta Materialia, 2008, 56, 4658-4672.	7.9	39
49	New relationships between relative density and grain size during solid-state sintering of ceramic powders. Acta Materialia, 2008, 56, 6273-6282.	7.9	45
50	Influence of Co-Doping on the Sintering Path and on the Optical Properties of a Submicronic Alumina Material. Journal of the American Ceramic Society, 2008, 91, 1703-1706.	3.8	37
51	Comparisons of grain size-density trajectory during spark plasma sintering and hot-pressing of zirconia. Materials Letters, 2008, 62, 4555-4558.	2.6	19
52	Spark plasma sintering of a commercially available granulated zirconia powder: I. Sintering path and hypotheses about the mechanism(s) controlling densification. Acta Materialia, 2007, 55, 3493-3504.	7.9	211
53	Apparent Activation Energy for the Densification of a Commercially Available Granulated Zirconia Powder. Journal of the American Ceramic Society, 2007, 90, 1246-1250.	3.8	62
54	Sintering Behavior and Optical Properties of Yttria. Journal of the American Ceramic Society, 2007, 90, 2698-2702.	3.8	53

#	Article	IF	CITATIONS
55	Influence of MgO or TiO2 doping on the sintering path and on the optical properties of a submicronic alumina material. Scripta Materialia, 2007, 56, 983-986.	5.2	28
56	Sintering of ceramic powders: Determination of the densification and grain growth mechanisms from the "grain size/relative density―trajectory. Scripta Materialia, 2007, 57, 137-140.	5.2	36
57	Sintering of an ultra pure α-alumina powder: I. Densification, grain growth and sintering path. Journal of Materials Science, 2007, 42, 6316-6324.	3.7	38
58	Compressive creep behavior in air of a slightly porous as-sintered polycrystalline α-alumina material. Journal of Materials Science, 2007, 42, 2807-2819.	3.7	11
59	Étude du frittage SPS d'une poudre de zircone ultrafine. Materiaux Et Techniques, 2007, 95, 235-239.	0.9	1
60	Influence of Co-Doping on the Sintering Map of an Ultra Fine and Ultra Pure Alpha Alumina Powder. Advances in Science and Technology, 2006, 45, 55.	0.2	1
61	Mechanical spectroscopy connected to creep and stress relaxation in a high resistant silicon nitride. Journal of the European Ceramic Society, 2002, 22, 2511-2516.	5.7	3
62	Compressive Creep and Stress Relaxation Kinetics in a High Purity Silicon Nitride Ceramics in the 1400-1650 °C Range. Key Engineering Materials, 2000, 171-174, 817-824.	0.4	2
63	Déformation du nitrure de silicium entre 1400 et 1700°C. Revue De Metallurgie, 2000, 97, 1047-1054.	0.3	0
64	Ductility and stress relaxation kinetics in a silicon nitride ceramic in the 1400–1650°C range. Journal of Materials Science Letters, 2000, 19, 1007-1010.	0.5	5
65	Observation of Different Interfaces in Silicon Nitride by HRTEM. Influence of the Microstructure on the Creep Properties Key Engineering Materials, 1997, 132-136, 559-562.	0.4	2
66	High temperature creep behaviour of ceramics. Journal of the European Ceramic Society, 1997, 17, 1647-1654.	5.7	28
67	Glassy grain-boundary phase crystallization of silicon nitride: Kinetics and phase development. Journal of Materials Science Letters, 1995, 14, 1362-1365.	0.5	13
68	High temperature anelastic behaviour of silicon nitride studied by mechanical spectroscopy. Acta Metallurgica Et Materialia, 1995, 43, 419-426.	1.8	36
69	Superplastic deformation of an alumina-zirconia matrix reinforced with SiC whiskers. Journal of the European Ceramic Society, 1992, 10, 13-20.	5.7	6